Remote Sensing of Suspended Particulate Matter in Himalayan Lakes

Authors: Giardino, Claudia, Oggioni, Alessandro, Bresciani, Mariano, and Yan, Huimin

Source: Mountain Research and Development, 30(2) : 157-168

Published By: International Mountain Society

URL: https://doi.org/10.1659/MRD-JOURNAL-D-09-00042.1

Mountain Research and Development (MRD)
An international, peer-reviewed open access journal
published by the International Mountain Society (IMS)
www.mrd-journal.org

MountainResearch
Systems knowledge

Remote Sensing of Suspended Particulate Matter in Himalayan Lakes

A Case Study of Alpine Lakes in the Mount Everest Region

Claudia Giardino[1], Alessandro Oggioni[2,3], Mariano Bresciani[1], and Huimin Yan[4]*

** Corresponding author: giardino.c@irea.cnr.it*

[1] Institute for Electromagnetic Sensing of the Environment, National Research Council, Consiglio Nazionale delle Ricerche–Istituto per il Rilevamento Elettromagnetico dell'Ambiente, via Bassini 15, Milano, Italy

[2] Ev-K2-CNR Committee, Via San Bernardino 145, 24126 Bergamo, Italy

[3] Institute of Ecosystems Studies, National Research Council, Consiglio Nazionale delle Ricerche–Istituto per il Rilevamento Elettromagnetico dell'Ambiente, Largo Tonolli 50, 28922 Verbania Pallanza, Italy

[4] Chinese Academy of Sciences–Institute of Geographical Sciences and Natural Resources Research, Beijing, PR China

This study presents satellite data and in situ measurements to estimate the concentration of suspended solids in high-altitude and remote lakes of the Himalayas. Suspended particulate matter (SPM) concentrations measured in 13 lakes to the south of Mount Everest (Nepal) in October 2008 and reflectance values of the Advanced Visible and Near Infrared Radiometer type 2 (AVNIR-2) onboard ALOS, acquired a few days after the fieldwork activities concluded, were combined to build a relationship (R^2 = 0.921) for mapping SPM concentrations in lakes of the Mount Everest region. The satellite-derived SPM concentrations were compared with in situ data (R^2 = 0.924) collected in the same period in 4 additional lakes, located to the north of Mount Everest (Tibet, China). The 13 water samples collected in lakes in Nepal were also used to investigate the absorption coefficients of particles $a_p(\lambda)$ and colored, dissolved organic matter $a_{CDOM}(\lambda)$, with the aim of parameterizing a bio-optical model. An accurate model (R^2 = 0.965) to estimate SPM concentrations from $a_p(\lambda)$ was found and could be adopted in the future for retrieving suspended solids from satellite imagery independently of ground measurements. In such a remote area, remote sensing was demonstrated to be a suitable tool to characterize the state of lakes, whose loads of suspended solids might be assumed to be direct and quick-responding indicators of deglaciation processes and glacier–lake interactions. As a macrodescriptor of water quality, the assessment of SPM in glacial lakes of the Himalayas might also be of interest for resource use in the downstream region.

Keywords: *Himalayan lakes; water color; suspended solids; glacier–lake interactions; remote sensing; ALOS AVNIR-2; Nepal.*

Peer-reviewed: *September 2009* ***Accepted:*** *February 2010*

Introduction

Global warming has resulted in a large-scale retreat of glaciers throughout the world (Oerlemans 2005). The evidence for this is particularly strong in high-altitude areas, such as the central Himalaya (Solomon et al 2007; Hambrey et al 2009; Quincey et al 2009; Ye et al 2009), where widespread recession is evident from the rapid growth in the number and size of glacial lakes (Chikita et al 2001; Quincey et al 2007; Bolch et al 2008; Tartari et al 2008; Wang et al 2008; Ye et al 2009).

Deglaciation processes are also revealed by the amount of suspended solids transported by glacier waters melting into the lake (Østrem et al 2005), with consequences for light propagation in the water body. If glacier water influx into a lake increases, then the maximum suspended particle size and particle number density will increase, and this affects light scattering. For decreased meltwater input, absorption because of water increases and the preferential red absorption because of water are enhanced. In lakes that have no glacial input, lake water is clear, and there is almost no scattering or absorption because of suspended matter (Kargel et al 2005). The recognition of lakes hydraulically connected to the glacier hydrological systems, hence full of silt (eg moraine-dammed supraglacial lakes), as opposed to those that are isolated (eg cirque lakes), would add value to studies (eg Tartari et al 2008) on processes of glacial-lake formation and expansion. Ultimately, these studies might contribute to an assessment of glacial lake hazard, because some moraine-dammed lakes may be unstable and potentially susceptible to sudden discharge of large

FIGURE 1 The study area in Himalaya. The map was developed based on an ALOS AVNIR-2 image acquired on 24 October 2008. The location of the sampled lakes are indicated by numbers: for the lakes sampled to the south of Mount Everest the cadastre numbers in Tartari et al (1997 and 2008) were used. The map also indicates main glaciers, peaks, and valleys in the Nepal–China border region.

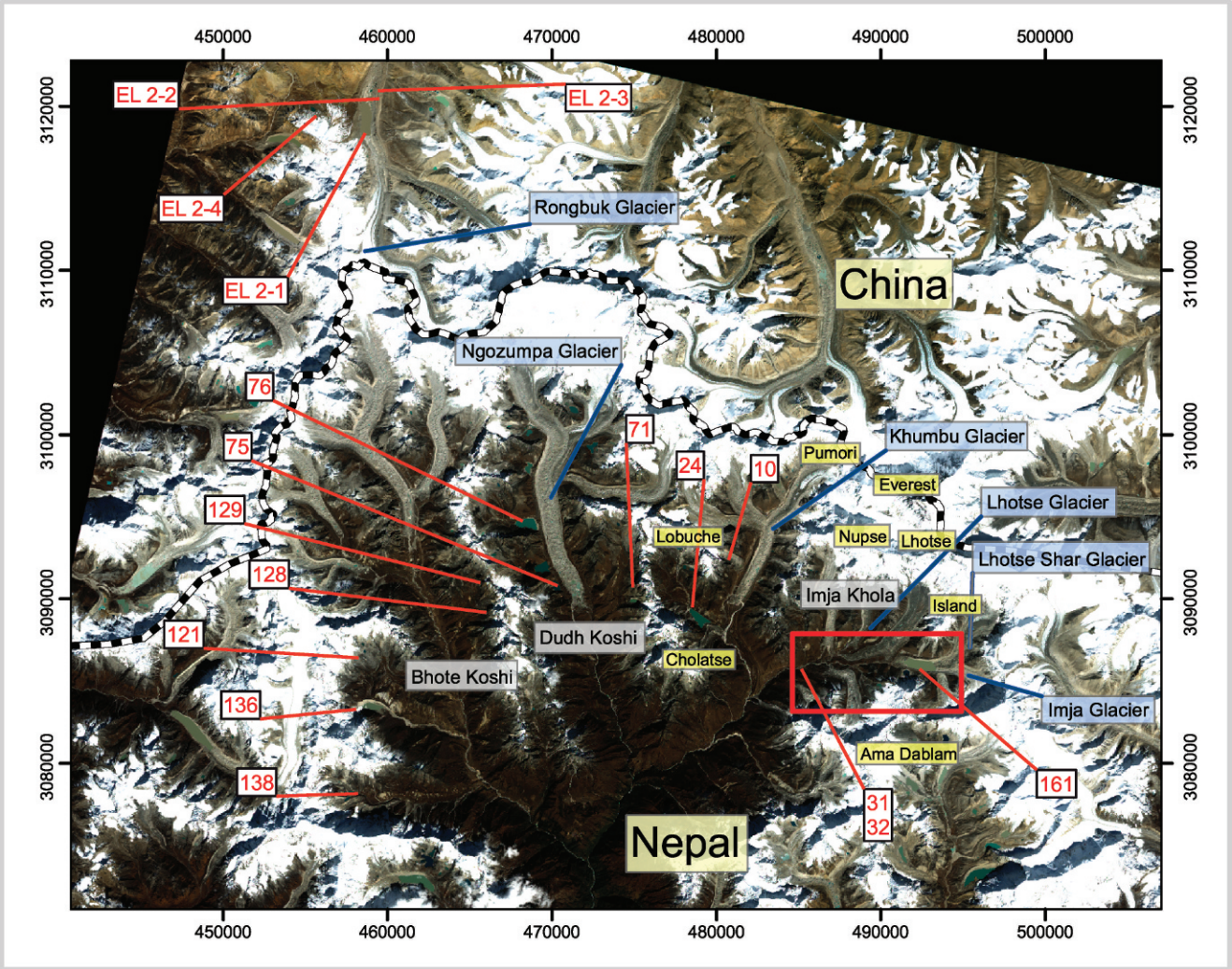

volumes of water and debris, which could cause floods hazardous to communities and infrastructure downstream (Richardson and Reynolds 2000; Kattelmann 2003; Bajracharya et al 2007; Quincey et al 2007; Bolch et al 2008).

Besides indicating the dynamics of the interaction between glaciers and lakes, suspended solids play a fundamental role in the aquatic system itself. They regulate the transport routes of all types of materials and contaminants in aquatic ecosystems (Wetzel 1983) and ultimately determine the primary productivity of water (Zhang et al 2008). As an indicator of water clarity (eg Secchi disk depth and water transparency, see Håkanson et al 2007), suspended solid concentration is also a macrodescriptor of water quality directly related to many variables of general use in lake management (Baban 1999). Water quality monitoring in the Himalayan region would contribute to proper management of some glacial lakes that could provide valuable water, energy, and tourism resources to local residents in the downstream regions (Komori 2008; Salerno et al 2008).

Suspended solids are traditionally measured by collecting water samples and then analyzing them in the laboratory. However, the extreme climate variations and the inaccessible terrain of the Himalayan region make it difficult to perform an assessment of suspended solids with traditional in situ methods. Remote sensing represents a useful tool for augmenting or replacing in situ methods and can be used to survey large areas regularly for dynamic monitoring.

TABLE 1 Characteristics of the sampled lakes with indication of their origin. (Table extended on next page.)

Valley	Lake no.	Origin	Altitude (m asl)	Sampling station (WGS84)	
				East	North
Imja Khola	10	Cirque	5080	481016	3093401
Imja Khola	24	Moraine-dammed	4520	479756	3088519
Imja Khola	31	Cirque	4680	484581	3084659
Imja Khola	32	Cirque	4660	484324	3084880
Duth Koshi	71	Supraglacial	4920	474797	3089746
Duth Koshi	75	Moraine-dammed	4740	470038	3091588
Duth Koshi	76	Moraine-dammed	4843	469255	3094264
Bhote Koshi	121	Cirque	5160	458401	3086228
Bhote Koshi	128	Cirque	4900	465306	3089599
Bhote Koshi	129	Cirque	5120	465592	3091165
Bhote Koshi	136	Moraine-dammed	4377	459920	3083263
Bhote Koshi	138	Moraine-dammed	4780	458166	3078208
Imja Khola	161	Supraglacial/moraine-dammed	5010	490806	3086106
Dingri County	EL 2–1	Supraglacial/moraine-dammed	5105	459120	3120594
Dingri County	EL 2–2	Supraglacial	5105	459010	3120974
Dingri County	EL 2–3	Supraglacial	5110	459270	3121304
Dingri County	EL 2–4	Supraglacial	5341	455480	3119864

Suspended solids are one of the parameters that can be measured successfully by means of remote sensing in inland waters (Lindell et al 1999 and references therein). Generally, 2 approaches can be used (Dekker et al 1995; Cracknell et al 2001) to estimate water quality parameters (including suspended solids) in lakes from satellite data:

- The semiempirical approach can be used when the degree of variation of spectral characteristics of water reflectance associated with the variation of parameters of interest is known (Härmä et al 2001). This knowledge is included in the statistical analysis by focusing on well-chosen spectral areas and appropriate wavebands used as correlates. The statistical relationships are then developed between satellite-derived water reflectance and corresponding concentrations of in situ data (water samples).
- In the analytical approach, the parameters of interest are related to the water reflectance by means of bio-optical models. Bio-optical models are mathematical equations that relate radiometric variables observed above or below the water surface (eg satellite-derived water reflectance) to the inherent optical properties (IOP) (ie absorption and back-scattering coefficients). The IOPs of each water component (ie absorption and back-scattering coefficients of colored dissolved organic matter (CDOM) and particle, the latter usually split in phytoplankton and detritus) are then related to concentrations of water quality parameters (eg suspended solids and $a_{CDOM}(440)$, the latter being the absorption coefficient at 440 nm of CDOM). The analytical method involves inverting all of the above relations to determine the concentrations of water quality parameters from satellite-derived water reflectance. An example of such an approach, by using Landsat data from Dutch lakes, can be found in Dekker et al (2001) for total suspended matter retrieval.

Quantitatively, the relationships developed to assess water quality within semiempirical approaches are sensor-dependent and may only apply to the data from which they are derived. Instead, well-calibrated and validated bio-optical models within the analytical

TABLE 1 Extended; na, not available. (First part of Table 1 on previous page.)

Valley	Lake no.	Area (km^2)	SPM (g/m^3)[a)]	$a_p(440)$ (m^{-1})[a)]	$a_{CDOM}(440)$ (m^{-1})[a)]
Imja Khola	10	0.017	0.63	0.011	0.4557
Imja Khola	24	0.536	6.69	0.141	1.0651
Imja Khola	31	0.057	1.70	0.050	0.4871
Imja Khola	32	0.006	0.69	0.022	0.8041
Duth Koshi	71	0.087	22.88	0.663	0.6881
Duth Koshi	75	0.413	3.07	0.111	0.7141
Duth Koshi	76	0.582	7.02	0.214	1.2677
Bhote Koshi	121	0.029	19.82	0.376	1.6010
Bhote Koshi	128	0.054	3.00	0.045	0.6166
Bhote Koshi	129	0.059	0.41	0.019	0.3488
Bhote Koshi	136	0.423	16.62	0.344	1.1293
Bhote Koshi	138	0.031	5.79	0.156	1.1418
Imja Khola	161	0.705	102.00	1.723	5.2505
Dingri County	EL 2–1	1.223	320.00	na	na
Dingri County	EL 2–2	0.016	14.00	na	na
Dingri County	EL 2–3	0.016	14.00	na	na
Dingri County	EL 2–4	0.003	0.5	na	na

[a)] The last 3 columns indicate the results of laboratory analysis performed on water samples.

approach are more general and may be applicable to every scene acquired over selected lakes independently of ground measurements. However, a great effort is needed to establish robust relationships between IOPs and concentrations of water quality parameters, because lakes are optically complex waters in which the relations between IOPs and concentrations of water components seem to have local-regional behavior (Kutser et al 2001) and may vary over time (Giardino et al 2007).

The purpose of this study was to measure the capability of satellite data to retrieve the suspended particulate matter (SPM) concentrations of glacial lakes in the Mount Everest region. The semiempirical approach was considered suitable to demonstrate the value of this technique in rapidly mapping SPM in lakes and studying the dynamics of interaction between glaciers and lakes. Moreover, the relations between the absorption coefficients of particles and CDOM with water quality parameters (ie SPM and CDOM), all derived from in situ measurements, were described in the perspective of bio-optical modeling. This is a preliminary step for implementing a remote-sensing–based procedure for water quality monitoring of Himalayan lakes.

Study area, data sources, and methods

The present investigation concerns the glacial lakes in the Himalayan region that extend to the north and south of Mount Everest at approximately 27°58′N; 86°45′E. The study area covers approximately 1300 km^2 and presents unique features, being surrounded on all sides by the highest mountain range on Earth. Within this area, 17 lakes were surveyed in September–October 2008 (Figure 1, Table 1). The lakes located in Nepal are indicated with the same numbers used by the lake cadastre of Sagarmatha National Park (SNP) (Tartari et al 1997; Tartari et al 2008), whereas, for the Chinese lakes, an arbitrary numeration was used. The lakes were distinguished in 3 categories, supraglacial, moraine-dammed, and cirque, according to both Tartari et al (2008) and field notes.

In the southern part (Nepal), the surveyed area is demarcated by the valley of the rivers Bhote Koshi, Dudh Koshi, and Imja Khola (Figure 1), which together drain into the Dudh Kosi river and afterward into the Ganges on the plain near Chatra. The surface area of the region is 1025 km^2 and covers 89% of the 1148 km^2 of SNP, located in the east of Nepal in a complex transition zone between

http://dx.doi.org/10.1659/MRD-JOURNAL-D-09-00042.1

FIGURE 2 Satellite-derived reflectance for the lakes sampled to the south of Mount Everest, in Nepal. 3 groups of spectra are distinguishable for increasing brightness; lower-reflectance spectra are indicated with blue lines; higher-reflectance spectra are indicated with light gray lines; in between are the medium-reflectance spectra. The embedded photos show the variation of colors for 3 lakes from dark blue to gray (in situ: top 3 photos; crop from AVNIR-2 image: 2 images below).

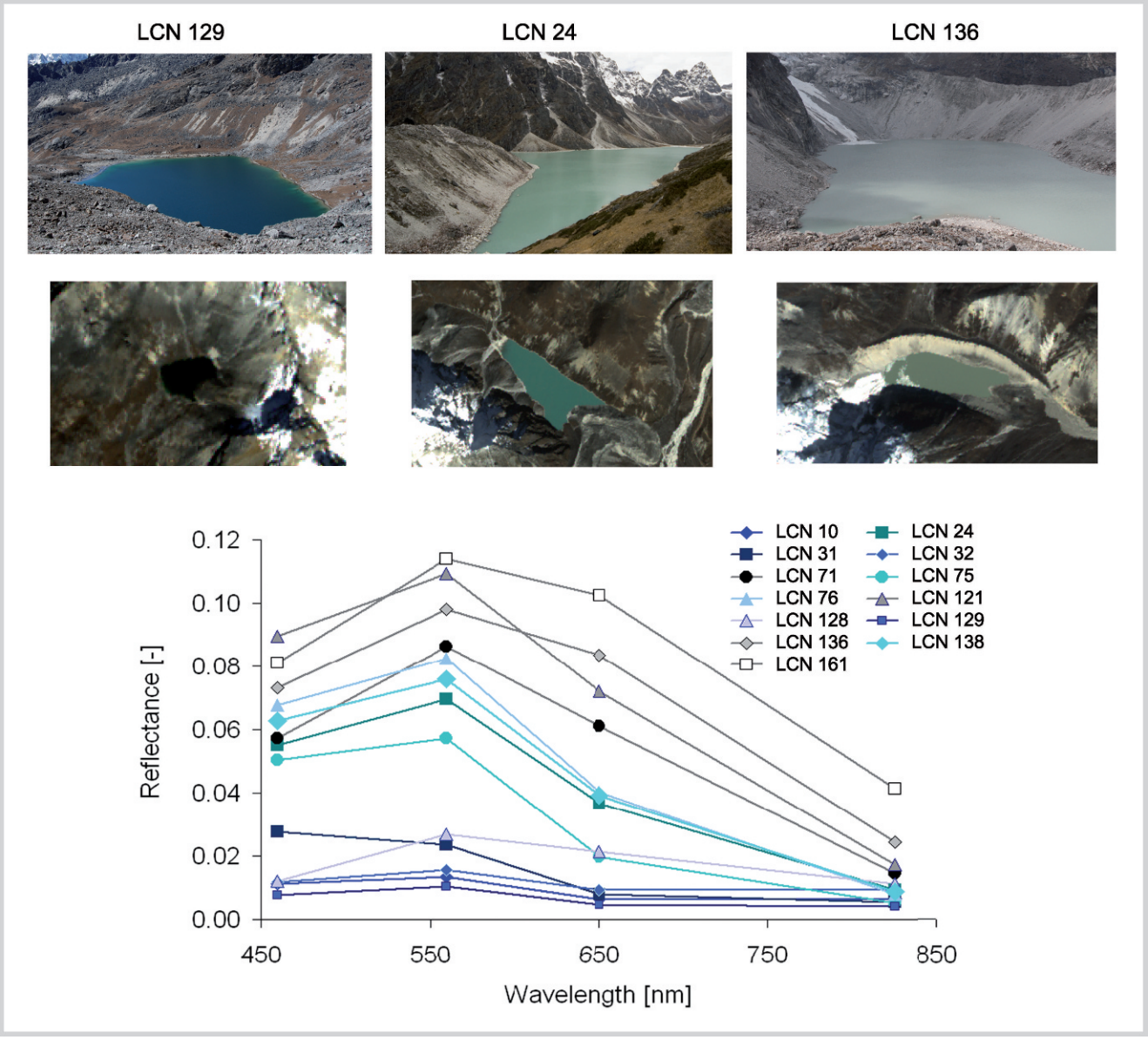

the high Himalaya and Tibet. The region is characterized by different geological units (Bortolami 1998), where the surface occupied by the lakes is very small compared with that occupied by glaciers, but the conditions are very different from valley to valley. In particular, 5 lakes (nos. 121, 128, 129, 136, and 138; Figure 1) were located in the Bhote Koshi Valley, which drains many small sub-basins in the western part of SNP and where more than 10 glacier formations are present. Of these 5 lakes, 2 are moraine-dammed lakes located in the immediate vicinity of the glacier (nos 136 and 138, Figure 1), 2 others are cirque lakes (nos 128 and 129, Figure 1), without any extensive glacier in their watersheds; the last lake (no. 121, Figure 1) is a small lake fed by a glacier located about 200 m above it. The other 3 lakes (nos. 71, 75, and 76; Figure 1) were located in the Dudh Koshi Valley, which is

FIGURE 3 (A) Natural logarithmic of SPM concentrations versus AVNIR-2 atmospherically corrected reflectance data ($R_{VIS-NIR}$). The regression line was used to map SPM concentrations from satellite data in the whole image; (B) comparison of satellite-derived and in situ measured SPM concentrations for the 4 lakes in China. In both plots symbols change according to water colors (hence to water reflectance and SPM concentrations): diamonds for dark blue lakes; squares for turquoise lakes; triangles for light gray lakes.

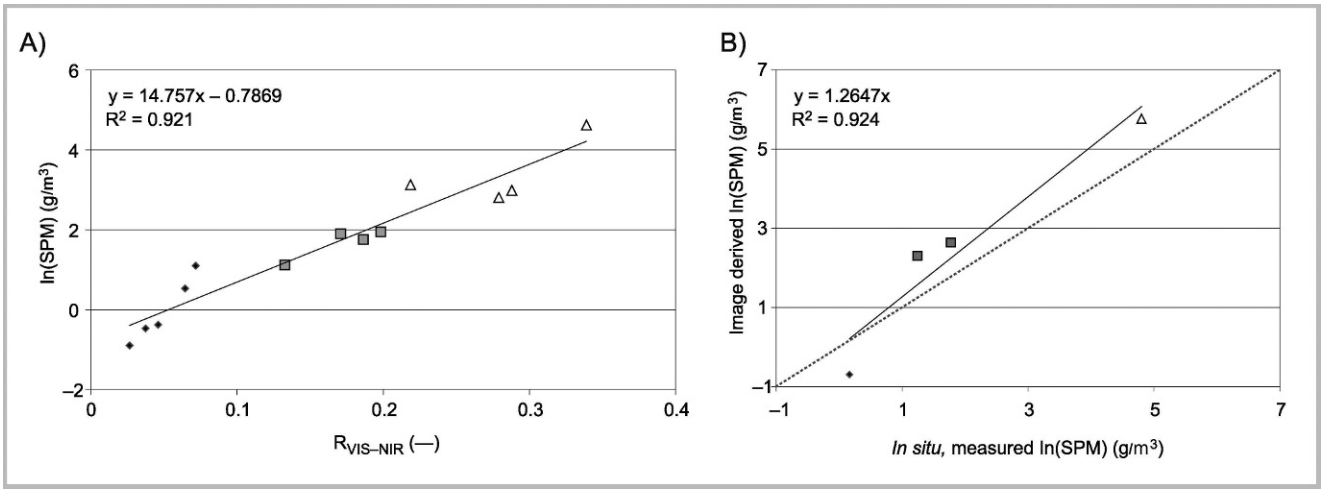

drained by the 25-km-long Ngozumpa Glacier. This valley contains an interesting group of later moraine-dammed lateral lakes. The remaining 5 lakes (nos. 10, 24, 31, 32, and 161; Figure 1) were located in the valley of Imja Khola where geomorphological conditions are more diversified. Of these, 3 were cirque lakes (nos. 10, 31, and 32; Figure 1). The fourth lake was Imja Lake (no. 161, Figure 1), a moraine-dammed lake, which began to grow after 1962 (Bolch et al 2008), fed by the Imja and Lhotse Shar glaciers. Toward the west, the large moraine-dammed Chola Lake (no. 24, Figure 1) was sampled. The lake drains the south side of Lobuche Peak and the northern icy side of the Cholatse and Taboche mountains.

In the northern part (Tibet, China), the study area is located in Dingri County, where the unique and various geographic conditions and the sensitive and vulnerable environment make it a perfect site for investigating changes in water quality and the dynamic process of glacial lakes in the context of climate change. Most of the lakes are located in the valleys close to the glaciers. They are formed by the accumulation of vast amounts of water from the melting of snow and ice cover and by blockage of end moraines. In particular, the investigated lakes were located in the Rongbuk river catchment, on the northern slopes of Mount Everest. The Rongbuk River is fed by the Rongbuk Glacier, which is the largest glacier in the catchment (Ye et al 2009). Many supraglacial lakes developed on the glacier terminus. The sampled lakes include 4 supraglacial lakes (nos. EL 2–1, EL 2–2, EL 2–3, and EL 2–4; Figure 1), among them the largest (EL 2–1, 1223 km^2, Figure 1 and Table 1) is also moraine dammed.

Field data

Two sets of fieldwork activities were performed in the study area to sample the lakes to the north and south of Mount Everest. The lakes to be sampled were selected before the campaigns according to (1) the color variability observed in pseudo true color composites of a Landsat image (path/row 140/41, acquired on 30 October 2000), (2) their size (preferably more than 3 × 3 Landsat pixels, ie 0.0081 km^2), and (3) their accessibility. A total of 17 lakes were sampled: 4 by the team that visited the Chinese lakes between 8 and 23 September 2008, and 13 by the team that surveyed the lakes in Nepal from 11–21 October 2008. The 17 lakes were located at an average altitude of 4900 m, with an average surface of 0.25 km^2 (Table 1).

In each lake, water samples for absorption measurements and water quality concentrations were collected at the topmost water layer (about 1 m). When depending on the amount of particles found, different volumes of water (from 1.5–4 L) were filtered. The samples were filtered in situ by the team working in Nepal, whereas the team that operated in the northern part conserved the samples below 4°C until they could be processed in the laboratory. In Nepal, additional water volumes were collected from each lake to determine the absorption coefficients of particles $a_p(\lambda)$, the absorption coefficients of CDOM $a_{CDOM}(\lambda)$, and the concentration of CDOM [ie $a_{CDOM}(440)$]. The concentrations of SPM were determined with the gravimetric method by both teams (Strömbeck and Pierson 2001); the absorption coefficients $a_p(\lambda)$ and $a_{CDOM}(\lambda)$ of water samples collected in Nepal were determined according to Fargion and Mueller (2000).

http://dx.doi.org/10.1659/MRD-JOURNAL-D-09-00042.1

FIGURE 4 (A) Map of SPM concentrations in lakes located in Imja Kola valley (see box in Figure 1). In dark blue the lakes with SPM < 3 g/m^3; in turquoise the lakes with SPM from 3–16 g/m^3, in light gray the lakes with SPM > 16 g/m^3. The largest lake on the map is Imja Lake (no. 161, Figure 1), the 2 small lakes in the eastern part are 2 cirque lakes (nos. 31 and 32, Figure 1) sampled during the fieldwork activities. The circular lake south of Imja Lake with low SPM concentration is Amphulaptse Lake. (B) Zoom on Imja Lake where SPM concentrations are mapped with a color table describing the spatial variation of SPM within the lake.

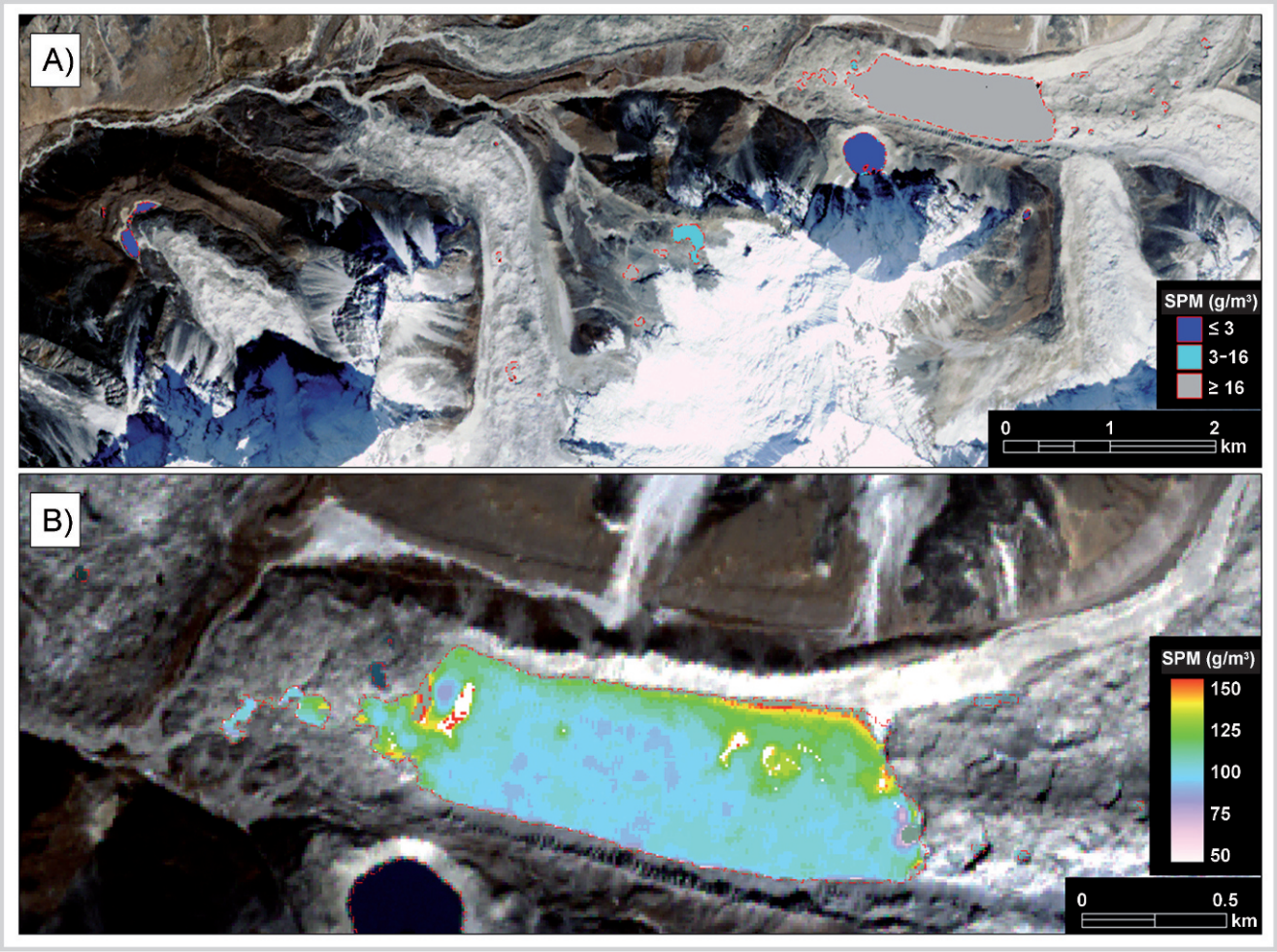

Satellite data

Satellite data were obtained by the Advanced Visible and Near Infrared Radiometer type 2 (AVNIR-2) onboard ALOS, a Japanese Earth Observation satellite launched in January 2006. AVNIR-2 is a multispectral radiometer for observing land and coastal zones with a 10-m spatial resolution, a 70-km swath width (at nadir), and a revisiting time of 46 days. It has 3 bands in the visible (VIS) range (wavelength centers of 420, 520 and 610 nm; bandwidths of 80 nm) and 1 band in the near-infrared (NIR) (wavelength center 760 nm, bandwidth 130 nm). AVNIR-2 data investigated in this study were acquired on 24 October 2008 (Scene ID ALAV2A146473040), just at the end of fieldwork activities, in a cloudless sky. The image was acquired at the end of the monsoon season before the first big snowfall.

Image data were orthorectified and corrected for the atmospheric effects by using the 6S code (Vermote et al 1997). The code was run according to nadir viewing and illumination conditions of the sun's zenith of 43° and the sun's azimuth of 156°. The aerosol optical depth at 550 nm was set to the mean value of the month (0.02) derived from the Ev-K2-CNR AERONET station. A threshold of band 4 to band 1 ratio was applied for binary discrimination to classify water pixels from the other surfaces. The threshold was chosen according to the spectral properties of water in terms of brightness (lower reflectance in comparison with other surfaces) and shape (lower reflectance in the NIR than in the blue wavelengths). The cast shadow areas wrongly classified as water body (commission error of 7.2%) were removed by visual inspection.

The 6S-derived reflectances are showed in Figure 2 for the lakes sampled to the south of Mount Everest. Three groups of spectra with increasing degrees of brightness are clearly distinguished with consequences of water color. By integrating the water reflectance in the whole range of AVNIR-2 bands, from VIS to NIR wavelengths ($R_{VIS\text{-}NIR}$), it can be observed that higher reflectance spectra ($R_{VIS\text{-}NIR} > 20\%$) correspond to lakes whose color, in the pseudo true color AVNIR-2 image, appears gray (nos. 71, 121, 136, and 161). However, lower reflectance spectra ($R_{VIS\text{-}NIR} < 10\%$) correspond to lakes whose color appears dark blue (nos. 10, 31, 32, 128, and 129). In between ($10\% \leq R_{VIS\text{-}NIR} \leq 20\%$), there is a group of spectra that correspond to lakes whose color appears turquoise (nos. 24, 75, 76, and 138). This can also be confirmed visually (Figure 2, embedded photos).

Results and discussion

Suspend particulate matter

Widely variable SPM concentrations were encountered in the study area (Table 1); the maximum (320 g/m^3) and minimum (0.41 g/m^3) SPM concentrations were measured in lakes EL 2–1 and no. 129, to the north and to the south of Mount Everest, respectively. Overall, in cirque lakes the SPM concentrations were lower than 3 g/m^3, whereas supraglacial and moraine-dammed lakes were characterized by wide variations in SPM concentrations, with values greater than 100 g/m^3 in the 2 largest sampled lakes (nos. 161 and EL 2–1). However, a few exceptions were observed: in cirque lake no. 121, the SPM concentration was about 20 g/m^3, whereas in the supraglacial lake EL 2–3 in China the SPM concentration was only 0.5 g/m^3. Field notes indicated that lake no. 121 was receiving water from a glacier located approximately 200 m above it; whereas the supraglacial lake EL 2–3 was a small, shallow, and clear pond above the Rongbuk Glacier.

The SPM concentrations measured in lakes in Nepal (see Figure 2 and Table 1) were used to establish the relationship with satellite data. The AVNIR-2 derived reflectance $R_{VIS\text{-}NIR}$ was considered the dependent variable. This rough estimation of lake albedo was considered suitable to represent the intensity of water reflectance and the observed desaturation of lake colors from dark-blue to gray. The relationship between SPM and $R_{VIS\text{-}NIR}$ is shown in Figure 3A; symbols are used to distinguish the samples for increasing $R_{VIS\text{-}NIR}$ values according to 3 clusters (Figure 2): $R_{VIS\text{-}NIR} < 10\%$, $10\% \leq R_{VIS\text{-}NIR} \leq 20\%$, and $R_{VIS\text{-}NIR} > 20\%$. A direct correlation between SPM and $R_{VIS\text{-}NIR}$ with a high degree of fit ($R^2 = 0.921$) was retrieved, thus the regression line (Figure 3A) was applied to each lake pixel of AVNIR-2 $R_{VIS\text{-}NIR}$ data to generate a map of SPM concentrations for all the whole lakes in the study area. The satellite-derived SPM concentrations were compared with in situ data, measured in the 4 lakes located in the northern part of the study area (nos. EL 2–1, EL 2–2, EL 2–3, and EL 2–4; Figure 1). A high degree of fitting was found ($R^2 = 0.924$) (Figure 3B), despite an underestimation of lower values and an overestimation of higher concentrations detected. The results confirm the capacity of the technique to describe a wide range of SPM concentrations and to quickly locate the lakes according to the 3 classes of SPM concentrations (dark blue, turquoise, and gray).

The map of SPM for a spatial subset of the study area is shown in Figure 4A (see box in Figure 1), in the region of the Imja Kola valley. The SPM concentrations were mapped with color codes comparable with SPM concentration ranges, which also correspond to the brightness of water reflectance: in blue, the lakes in which SPM is lower than 3 g/m^3 (and $R_{VIS\text{-}NIR} < 10\%$); in turquoise, the lakes in which SPM ranges from 3–6 g/m^3 ($10\% \leq R_{VIS\text{-}NIR} \leq 20\%$); in gray, the lakes in which SPM concentration is greater than 16 g/m^3 ($R_{VIS\text{-}NIR} > 20\%$). The map shows a sequence of several lakes whose SPM concentrations varied significantly. In the western part, the 2 cirque lakes nos. 31 and 32 (see Figure 1 and Table 1) were characterized by low concentrations of SPM ($\leq$3 g/m^3). When moving toward the east, 2 lakes with significantly dissimilar SPM concentrations are distinguishable. In Amphulaptse Lake (circular shape) the concentrations of SPM were lower than 3 g/m^3, which indicated the absence of glacier–lake interactions. This behavior was also described by Bolch et al (2008), who did not observe any change in the lake's size from 1962–2003. Finally, the large Imja Lake (no. 126, Figure 1) was characterized by higher concentrations of SPM, which indicated that it has been receiving silt inputs from the glacier. The result was in agreement with the progression of Imja Lake, whose growth has been carefully analyzed (Yamada 1998; Quincey et al 2005; Bajracharya et al 2007; Bolch et al 2008; Hambrey et al 2009). For Imja Lake, the SPM map was further investigated by defining more-appropriate color ranges for appreciating the spatial distribution of suspended solids (Figure 4B). The SPM concentrations mainly ranged between 75 and 125 g/m^3, with higher concentrations observed toward the northern part, whereas any significant pattern was instead visible, moving from the glacier tongue toward the dam. The satellite-derived SPM concentrations were comparable with Chikita (2004): in his study, in situ measured suspended sediment concentrations at the surface were about 80 g/m^3 (they reached 100 g/m^3 toward the lake bottom), which suggests that the silt inputs from the glacier did not vary significantly.

Absorption coefficients

The values of the normalized $a_p(440)/a_{tot}(440)$ and $a_{CDOM}(440)/a_{tot}(440)$ [with $a_{tot}(440) = a_p(440) + a_{CDOM}(440)$] for the samples collected in 13 lakes in Nepal are shown in Table 2. The statistics are computed

TABLE 2 Global and subcluster statistics for the absorption coefficients at 440 nm of particles $a_p(440)$ and CDOM $a_{CDOM}(440)$ with respect to the total absorption coefficients $a_{tot}(440)$.[a)]

Group	N	$a_p(440)/a_{tot}(440)$				
		Min value	Max value	Average	SD	VC (%)
Dark blue	5	0.0228	0.0930	0.0523	0.0293	56.07
Turquoise	4	0.1901	0.4909	0.2904	0.1359	46.79
Gray	4	0.1169	0.1442	0.1289	0.0127	9.86
All	**13**	**0.0228**	**0.4909**	**0.1491**	**0.1250**	**83.84**

TABLE 2 Extended.

Group	N	$a_{CDOM}(440)/a_{tot}(440)$				
		Min value	Max value	Average	SD	VC (%)
Dark blue	5	0.9070	0.9772	0.9477	0.0293	3.10
Turquoise	4	0.5091	0.8099	0.7096	0.1359	19.14
Gray	4	0.8558	0.8831	0.8711	0.0127	1.46
All	**13**	**0.5091**	**0.9772**	**0.8509**	**0.1250**	**14.69**

[a)] Min, minimum; Max, maximum; SD, standard deviation; VC, variation coefficient in percentage.

according to the 3 groups of lakes, previously defined according to $R_{VIS\text{-}NIR}$ values and SPM ranges: dark blue, turquoise, and gray lakes. The average value of $a_p(440)$ is greatest in turquoise lakes (0.29), whereas the average value of $a_p(440)$ reaches the minimum (0.052) in dark-blue lakes. On the contrary, the average normalized value of $a_{CDOM}(440)$ was higher in the dark-blue lakes (0.948) than in turquoise lakes (0.710). Although the range of variability did not vary significantly, these results suggest that, in the clearest lakes, the main absorption component was CDOM, whereas, in turquoise lakes, it was particles. The gray lakes stay in between, which indicated that CDOM and particles equally contributed to the absorption of light.

Similarly, all sampled lakes present a small range of variability with regard to the slopes of both particle (S_p) and CDOM (S_{CDOM}); these slopes being the scalar used to model the well-known (eg Babin et al 2003) exponential function: $a_i(\lambda) = a_i(440)e^{-Si}$, where i represents the particle "p" and CDOM, respectively. As showed in Table 3, the average values of S_p and S_{CDOM}, are 0.0116 and 0.0093, respectively; the latter being comparable with S_{CDOM} values found both in lakes (Strömbeck and Pierson 2001; Ma et al 2006) and in coastal waters (Babin et al 2003).

The absorption coefficients of $a_p(440)$ and $a_{CDOM}(440)$ were then analyzed to find their relationship with SPM and S_{CDOM}, respectively, under the perspective of parameterizing a bio-optical model for the study area. The relationship between $a_p(440)$ and SPM concentrations (see Table 1), whose strength ($R^2 = 0.965$) indicates that it can be applied in a bio-optical model to relate the absorption coefficient of particles to SPM concentrations, is shown in Figure 5A. With respect to CDOM, we found no significant results in investigating the inverse relationship that may exist between $a_{CDOM}(440)$ (see Table 1) and S_{CDOM} (Carder et al 1989; see Figure 5B). Therefore, in implementing a bio-optical model, the relationship between and $a_{CDOM}(\lambda)$ and $a_{CDOM}(440)$ should be a function of a constant slope S_{CDOM} (Dekker et al 2001). The results suggest that both SPM and CDOM could be obtained by inverting the bio-optical model, even though in situ data would be necessary to investigate the back-scattering coefficient of particles, which is needed to fully parameterize the bio-optical model. The technique then would simultaneously provide an assessment of SPM and CDOM (Brando and Dekker 2003).

Conclusions

This study demonstrated how ALOS AVNIR-2 satellite data may be used to retrieve SPM concentrations in high altitude lakes: the lakes are characterized by wide variations in SPM concentrations, ie from less than 1 g/m^3 to more than 300 g/m^3. The semiempirical approach was considered suitable to assess SPM concentrations in the study area. A robust relationship was developed ($R^2 = 0.921$) by comparing atmospherically corrected reflectance data, integrated in the VIS and NIR

http://dx.doi.org/10.1659/MRD-JOURNAL-D-09-00042.1

TABLE 3 Global and subcluster statistics for the spectral slopes of particle and CDOM.[a)]

Cluster	N	S_p (440)				
		Min value	Max value	Average	SD	VC (%)
Dark blue	5	0.0097	0.0125	0.0110	0.0011	9.77
Turquoise	4	0.0104	0.0137	0.0124	0.0014	11.54
Gray	4	0.0106	0.0124	0.0115	0.0007	6.31
All	**13**	**0.0097**	**0.0137**	**0.0116**	**0.0012**	**10.21**

TABLE 3 Extended.

Cluster	N	S_{CDOM} (440)				
		Min value	Max value	Average	SD	VC (%)
Dark blue	5	0.0075	0.0097	0.0089	0.0009	10.52
Turquoise	4	0.0086	0.0109	0.0093	0.0011	11.86
Gray	4	0.0092	0.0106	0.0097	0.0006	6.23
All	**13**	**0.0075**	**0.0109**	**0.0093**	**0.0009**	**9.65**

[a)] Min, minimum; Max, maximum; SD, standard deviation; VC, variation coefficient in percentage.

wavelength range, with SPM concentrations, sampled in 13 lakes south of Mount Everest (Nepal). The satellite-derived SPM concentrations were comparable with in situ data ($R^2 = 0.924$) collected in 4 lakes north of Mount Everest (Tibet, China). The results confirmed the capacity of this technique to retrieve a wide range of SPM concentrations and to quickly locate the lakes according to 3 classes of SPM concentrations. In 2 large ice-contact lakes (no. 161, Imja in Nepal, and EL 2–1 in China), the amount of silt was found to be particularly high (SPM > 100 g/m^3), which indicated that the lakes are hydraulically connected to the glaciers. The results are in agreement with recent findings describing the dramatic retreat of the Rongbuk and Imja glaciers, which has resulted in the rapid expansions of the EL 2–1 (Ye et al 2009) and Imja (Bolch et al 2008) lakes, respectively.

The study was complemented by the analysis of absorption coefficients of particles and CDOM. The

FIGURE 5 (A) Scatterplot of $a_p(440)$ as a function of SPM for the 13 lakes, sampled in Nepal; (B) scatterplot of S_{CDOM} as a function of $a_{CDOM}(440)$ for the 13 lakes, sampled in Nepal.

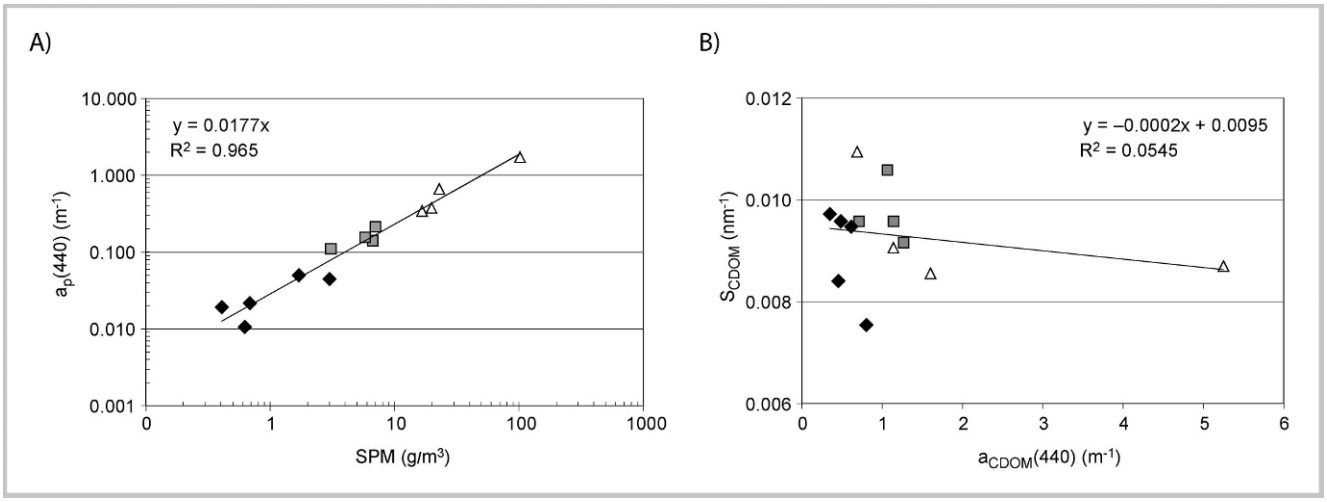

http://dx.doi.org/10.1659/MRD-JOURNAL-D-09-00042.1

results indicated a direct correlation between SPM and absorption of particles, with an almost complete absence of particles in clear-blue waters where the main absorption component was instead CDOM. The absorption coefficients were investigated as a preliminary step toward the goal of bio-optical modeling, which would allow remote sensing–based techniques to assess SPM concentrations independently of ground measurements (Zhang et al 2008). Moreover, the technique would simultaneously provide an assessment of CDOM, whose impact on water quality is not secondary, being a major structuring component of lake ecosystems and protecting the aquatic biota from ultraviolet solar radiation (Kutser et al 2005). The availability of a bio-optical model, together with time-series satellite images, normalized by illumination and atmospheric effects (as AVNIR-2 image used in this study), would make it possible to assess water quality in such a remote area synoptically and at different periods. Nevertheless, operational sensors with the spatial resolution of ALOS AVNIR-2 but improved temporal resolution are needed for implementing continuous monitoring programs. Such a requirement could be fulfilled by the recently launched RapidEye Satellite with a spectral configuration comparable with AVNIR-2.

The technique presented in this study might help to explain the processes of glacial lake formation and expansion, with emphasis on those processes characterized by rapid growth in the number and dimensions of glacial lakes that may generate catastrophic outburst floods (Kattelmann 2003). Being a macrodescriptor of water quality, the assessment of SPM in glacial lakes of the Himalayan region might also be of interest for resource use in the downstream region. Water quality measurements (both SPM and CDOM) in Himalayan lakes might also receive increasing attention in the wider scientific community. High-altitude lakes are regarded as potentially sensitive ecosystem indicators of global change because of their cold and dilute abiotic environment, low biodiversity, and considerable water clarity ranges, poor functional redundancy, and relative lack of local human perturbation (Skjelkvåle and Wright 1998; Sommaruga 2001; Battarbee et al 2002; Psenner et al 2002; Rogora et al 2008).

ACKNOWLEDGMENTS

This publication was produced within the framework of the project "Institutional Consolidation for the Coordinated and Integrated Monitoring of Natural Resources towards Sustainable Development and Environmental Conservation in the Hindu Kush–Karakoram–Himalaya Mountain Complex," financed by the Italian Ministry of Foreign Affairs–DGCS. ALOS AVNIR-2 data were acquired within the ESA AO553 MELINOS Project. Ev-K2-CNR AERONET data were provided by G.P. Gobbi. We are very grateful to T.C. Sherpa, Lax-Man, and Pema for their help in the fieldwork activities, and to G. Tartari, M. Gallo, and A. De Paolis for the sampling activities in the Sagarmatha National Park. We thank M.T. Melis and A. Lami for coordinating our research activities within the HKKH Project. We are grateful to N. Dwyer and A. Thean for the English revision of the manuscript. Constructive comments from 2 anonymous reviewers were greatly appreciated.

REFERENCES

Baban SMJ. 1999. Use of remote sensing and geographical information systems in developing lake management strategies. *Hydrobiologia* 395/396: 211–226.

Babin M, Stramski D, Ferrari GM, Claustre H, Bricaud A, Obolensky G, Hoepffner N. 2003. Variations in the light absorption coefficients of phytoplankton, nonalgal particles, and dissolved organic matter in coastal waters around Europe. *Journal of Geophysical Research* 108:3211:4.1–4.20.

Bajracharya B, Shrestha AB, Rajbhandari L. 2007. Glacial lake outburst floods in the Sagarmatha Region. *Mountain Research and Development* 27:336–344.

Batterbee RW, Thompson R, Catalan J, Grytnes JA, Birks HJB. 2002. Climate variability and ecosystem dynamics of remote alpine and arctic lakes: The MOLAR project. *Journal of Paleolimnology* 28:1–6.

Bolch T, Buchroithner MF, Peters J, Baessler M, Bajracharya A. 2008. Identification of glacier motion and potentially dangerous glacial lakes in the Mt Everest region/Nepal using spaceborne imagery. *Natural Hazards Earth System Sciences* 8:1329–1340.

Bortolami G. 1998. Geology of the Khumbu Region, Mt Everest, Nepal. *Memorie Istituto Italiano di Idrobiolgia* 57:41–49.

Brando VE, Dekker AG. 2003. Satellite hyperspectral remote sensing for estimating estuarine and coastal water quality. *IEEE Transaction on Geoscience and Remote Sensing* 41:1378–1387.

Carder KL, Steward RG, Harvey GR, Ortner PB. 1989. Marine humic and fulvic acids: Their effects on remote sensing of ocean chlorophyll. *Limnology and Oceanography* 34:68–81.

Chikita K. 2004. The expansion mechanism of Himalayan supraglacial lakes: Observations and modeling. *Himalayan Journal of Sciences* 2(4):118–120.

Chikita K, Jha J, Yamada T. 2001. Sedimentary effects on the expansion of a Himalayan supraglacial lake. *Global and Planetary Change* 28:23–34.

Cracknell AP, Newcombe SK, Black AF, Kirby NE. 2001. The ADMAP (algal bloom detection, monitoring and prediction) Concerted Action. *International Journal of Remote Sensing* 22:205–247.

Dekker AG, Malthus TJ, Hoogenboom HJ. 1995. The remote sensing of inland water quality. *In*: Danson FM, Plummer SE, editors. *Advances in Environmental Remote Sensing*. Chichester, United Kingdom: Wiley, pp 123–142.

Dekker AG, Vos RJ, Peters SWM. 2001. Comparison of remote sensing data, model results and in situ data for total suspended matter (TSM) in the southern Frisian lakes. *Science of the Total Environment* 268:197–214.

Fargion GS, Mueller JL. 2000. Trip Report. Ocean optics protocols for satellite ocean color sensor validation, Revision 2, NASA/TM-2000-209966, Greenbelt, MD, USA.

Giardino C, Brando VE, Dekker AG, Strömbeck N, Candiani G. 2007. Assessment of water quality in Lake Garda (Italy) using Hyperion. *Remote Sensing of Environment* 109:183–195.

Håkanson L, Bryhn AC, Blenckner T. 2007. Operational effect variables and functional ecosystem classifications: A review on empirical models for aquatic systems along a salinity gradient. *International Review of Hydrobiology* 92(3): 326–357.

Hambrey MJ, Quincey DJ, Glasser NF, Reynolds JM, Richardson SJ, Clemmens S. 2009. Sedimentological, geomorphological and dynamic context of debris-mantled glaciers, Mount Everest (Sagarmatha) region, Nepal. *Quaternary Science Reviews* 28:1084.

Härmä P, Vepsäläinen J, Hannonen T, Pyhälahti T, Kämäri J, Kallio K, Eloheimo K, Koponen S. 2001. Detection of water quality using simulated satellite data and semi-empirical algorithms in Finland. *The Science of the Total Environment* 268(1–3):107–121.

Kargel J, Abrams M, Bishop M, Bush A, Hamilton G, Jiskoot H, Kääb A, Kieffer HH, Lee EM, Paul F, Rau F, Raup B, Shroder JF, Soltesz D, Stainforth D, et al. 2005. Multispectral imaging contributions to global land ice measurements from space. *Remote Sensing of Environment* 99:187–219.

http://dx.doi.org/10.1659/MRD-JOURNAL-D-09-00042.1

Kattelmann R. 2003. Glacial lake outburst floods in the Nepal Himalaya: A manageable hazard? *Natural Hazards* 28:145–154.
Komori J. 2008. Recent expansions of glacial lakes in the Bhutan Himalayas. *Quaternary International* 184:177–186.
Kutser T, Herlevi A, Kallio KY, Arst H. 2001. A hyperspectral model for interpretation of passive optical remote sensing data from turbid lakes. *The Science of the Total Environment* 268:47–58.
Kutser T, Pierson DC, Kallio KY, Reinart A, Sobek S. 2005. Mapping lake CDOM by satellite remote sensing. *Remote Sensing of Environment* 2005:535–540.
Lindell T, Pierson D, Premazzi G, Zilioli E, editors. 1999. *Manual for monitoring European lakes using remote sensing techniques*. EUR Report 18665 EN. Luxemburg: Office for Official Publications of the European Communities.
Ma R, Tang J, Dai J, Zhang Y, Song Q. 2006. Absorption and scattering properties of water body in Taihu Lake, China: Absorption. *International Journal of Remote Sensing* 27:4277–4304.
Oerlemans J. 2005 Extracting climate signals from 169 glacier records. *Science* 308:675–677.
Østrem G, Haakensen N, Olsen HC. 2005. Sediment transport, delta growth and sedimentation in Lake Nigardsvatn, Norway. *Geografiska Annaler* 87:1243–1258.
Psenner R, Rosseland BO, Sommaruga R. 2002. Preface. High mountains lakes and stream: Indicators of a changing world. *Water, Air, and Soil Pollution: Focus* 2:1–4.
Quincey DJ, Lucas RM, Richardson SD, Glasser NF, Hambrey MJ, Reynolds JM. 2005. Optical remote sensing techniques in high-mountain environments: Application to glacial hazards. *Progress in Physical Geography* 29:475–505.
Quincey DJ, Luckman A, Benn D. 2009. Quantification of Everest region glacier velocities between 1992 and 2002, using satellite radar interferometry and feature tracking. *Journal of Glaciology* 55:596–606.
Quincey DJ, Richardson SD, Luckman A, Lucas RM, Reynolds JM, Hambrey MJ, Glasser NF. 2007. Early recognition of glacial lake hazards in the Himalaya using remote sensing datasets. *Global and Planetary Change* 56:137–152.
Richardson SD, Reynolds JM. 2000. Degradation of ice-cored moraine dams: Implications for hazard development. *In:* Nakawo M, Raymond CF, Fountain A, editors. *Debris-Covered Glaciers*. Publication 264, International Association of Hydrological Sciences (IAHS). Wallingford, United Kingdom: IAHS, pp. 187–197.
Rogora M, Massaferro J, Marchetto A, Tartari G, Mosello R. 2008. The water chemistry of some shallow lakes in northern Patagonia and their nitrogen status in comparison with remote lakes in different regions of the globe. *Journal of Limnology* 67:75–86.
Salerno F, Buraschi E, Bruccoleri G, Tartari G, Smiraglia C. 2008. Glacier surface-area changes in Sagarmatha National Park, Nepal, in the second half of the 20th century, by comparison of historical maps. *Journal of Glaciology* 54: 738–752.
Skjelkvåle BL, Wright RF. 1998. Mountain lakes: Sensitivity to acid deposition and global climate change. *Ambio* 27:280–286.
Solomon S, Qin D, Manning M, Chen Z, Marquis M, Averyt KB, Tignor M, Miller HL. 2007. *The Physical Science Basis. Contribution of Working Group I to the Fourth Assessment Report of the Intergovernmental Panel on Climate Change*. Cambridge, United Kingdom: Cambridge University Press.
Sommaruga R. 2001. The role of solar UV radiation in the ecology of alpine lakes. *Journal of Photochemistry and Photobiology B: Biology* 62:35–62.
Strömbeck N, Pierson E. 2001. The effects of variability in the inherent optical properties on estimations of chlorophyll a by remote sensing in Swedish freshwater. *Science of the Total Environment* 268:123–137.
Tartari G, Salerno F, Buraschi E, Bruccoleri G, Smiraglia C. 2008. Lake surface area variations in the north-eastern sector of Sagarmatha National Park (Nepal) at the end of the 20th century by comparison of historical maps. *Journal of Limnology* 67:139–154.
Tartari G, Tartari GA, Valsecchi S, Camusso M. 1997. Cadastre and hydrochemistry of high altitude lakes in the Mount Everest region. *Verhandlungen der Internationalen Vereinigung fur Theoretische und Angewandte Limnologie* 26:397–402.
Vermote EF, Tanrè D, Deizè JL, Herman M, Morcrette JJ. 1997. Second simulation of the satellite signal in the solar spectrum, 6S: An overview. *IEEE Transactions on Geoscience and Remote Sensing* 35:675–686.
Wang X, Liu SY, Guo WQ, Xu JL. 2008. Assessment and simulation of glacier lake outburst floods for Longbasaba and Pida lakes, China. *Mountain Research and Development* 28(3/4):310–317.
Wetzel R. 1983. *Limnology*. Philadelphia, PA: Saunders.
Yamada T. 1998. *Glacier Lake and its Outburst Flood in the Nepal Himalaya*. Monograph no. 1. Tokyo, Japan: Data Center for Glacier Research, Japanese Society of Snow and Ice.
Ye Q, Zhong Z, Kang S, Stein A, Wei Q, Liu J. 2009. Monitoring glacier and supra-glacier lakes from space in Mt Qomolangma region of the Himalayas on the Tibetan Plateau in China. *Journal of Mountain Sciences* 6:211–220.
Zhang B, Li J, Shen Q, Chen D. 2008. A bio-optical model based method of estimating total suspended matter of Lake Taihu from near-infrared remote sensing reflectance. *Environmental Monitoring Assessment* 145:339–347.